



VCU

Virginia Commonwealth University
VCU Scholars Compass

Electrical and Computer Engineering Publications

Dept. of Electrical and Computer Engineering

2008

Large pyroelectric effect in undoped epitaxial Pb(Zr,Ti)O₃ thin films on SrTiO₃ substrates

Bo Xiao

Virginia Commonwealth University, xiaob@vcu.edu

Vitaliy Avrutin

Virginia Commonwealth University, vavrutin@vcu.edu

Huiyong Liu

Virginia Commonwealth University

See next page for additional authors

Follow this and additional works at: http://scholarscompass.vcu.edu/egre_pubs

 Part of the [Electrical and Computer Engineering Commons](#)

Xiao, B., Avrutin, V., Liu, H., et al. Large pyroelectric effect in undoped epitaxial Pb(Zr,Ti)O₃ thin films on SrTiO₃ substrates. Applied Physics Letters, 93, 052913 (2008). Copyright © 2008 AIP Publishing LLC.

Downloaded from

http://scholarscompass.vcu.edu/egre_pubs/90

This Article is brought to you for free and open access by the Dept. of Electrical and Computer Engineering at VCU Scholars Compass. It has been accepted for inclusion in Electrical and Computer Engineering Publications by an authorized administrator of VCU Scholars Compass. For more information, please contact libcompass@vcu.edu.

Authors

Bo Xiao, Vitaliy Avrutin, Huiyong Liu, Ü. Özgür, Hadis Morkoç, and Changzhi Lu

Large pyroelectric effect in undoped epitaxial $\text{Pb}(\text{Zr},\text{Ti})\text{O}_3$ thin films on SrTiO_3 substrates

Bo Xiao,^{1,a)} Vitaliy Avrutin,¹ Huiyong Liu,¹ Ümit Özgür,¹ Hadis Morkoç,¹ and Changzhi Lu²

¹Department of Electrical and Computer Engineering, Virginia Commonwealth University, Richmond, Virginia 23284, USA

²School of Electronic Information and Control Engineering, Beijing University of Technology, Beijing 100022, People's Republic of China

(Received 4 June 2008; accepted 22 July 2008; published online 8 August 2008)

We have studied pyroelectric and ferroelectric properties of $\text{Pb}(\text{Zr},\text{Ti})\text{O}_3$ thin films grown epitaxially on $\text{SrTiO}_3(001)$ substrates by rf magnetron sputtering. The pyroelectric coefficient was measured in the temperature range from 280 to 370 K using the Byer–Roundy method. Values as high as 48 $\text{nC}/\text{cm}^2\text{K}$ have been obtained at 300 K. The PZT thin films exhibited a remanent polarization of 45–58 $\mu\text{C}/\text{cm}^2$. The improved pyroelectric coefficient was attributed to a high crystalline quality of the films, as revealed by x-ray diffraction that showed only (001)-oriented perovskite PZT phase and a ω -rocking curve full width at half maximum value as low as 4.2 arc min for 300 nm thick films. © 2008 American Institute of Physics.

[DOI: 10.1063/1.2969778]

Ferroelectric lead zirconate titanate $\text{Pb}(\text{Zr},\text{Ti})\text{O}_3$ (PZT) has been extensively studied theoretically and experimentally for decades. Its remarkable ferroelectric, pyroelectric, dielectric, and electro-optical properties offer great promise for various applications, such as nonvolatile memories, nonlinear optic devices, ultrasonic and motion sensors, infrared detectors, and microactuators.^{1,2} By virtue of large pyroelectric coefficient p of PZT, efforts have been extended to realize pyroelectric devices,^{3,4} capable of operating over a wide range of temperatures without a cooling system. Pyroelectricity is a coupled effect that relates the change in the electric displacement dD in a material to the change in the temperature dT :⁵ $dD=pdT$. To study and exploit the properties of PZT for pyroelectric device applications, high-quality PZT thin films are required. The similar crystal structure and good lattice match of PZT and strontium titanate (STO) make STO a suitable substrate material for growing high-quality PZT films.^{6,7} In addition, the close thermal expansion coefficients of PZT and STO can minimize the strain-induced secondary pyroelectric effect, and also allow growth in thick PZT films as well as processing at high temperatures. In this paper, we report the pyroelectric and ferroelectric properties of high-quality PZT thin films.

The PZT films of the morphotropic phase boundary (MPB) composition, $\text{Zr}:\text{Ti}=52:48$, were grown epitaxially by an off-axis rf magnetron sputtering system on $\text{STO}(001)$ substrates using a 3 in. diameter PZT target containing 10 mol % excess PbO to prevent Pb deficiency caused by high Pb volatility. During growth, Ar and O_2 gases were introduced into the growth chamber through mass flow controllers. Although the use of oxygen for growing oxide materials in rf sputtering enhances material oxidation, it causes resputtering of the growing films. Therefore, the oxygen flow rate was set at a relatively low level of 5 SCCM (SCCM denotes cubic centimeter per minute at STP) as compared to 30 SCCM of Ar. In addition, the off-axis sputtering geometry is intended to reduce resputtering. The total pressure of the

Ar and O_2 mixture gas was kept at 2 mTorr. The rf power was set at 120 W.

The crystal structure and orientation of as-deposited PZT films were characterized by high resolution x-ray diffraction (HRXRD). Under the conditions mentioned above, the substrate temperature was found to be a critical parameter controlling the formation of a perovskite phase. The PZT films grown at temperatures below 500 °C were dominated by the pyrochlore phase with only a minor presence of the perovskite phase. As the substrate temperature increased, the perovskite phase became dominant. The films grown at 700 °C showed only XRD peaks corresponding to the perovskite phase (700 °C is the maximum substrate temperature attainable in our sputtering system), as seen from the symmetrical 2θ - ω HRXRD scan shown in the inset of Fig. 1(a). The pattern is dominated by a (001) reflection from the STO substrate at 22.75° and a peak at 21.46° that is very close to the 2θ angle of (001) reflection from bulk PZT (21.414°, accord-

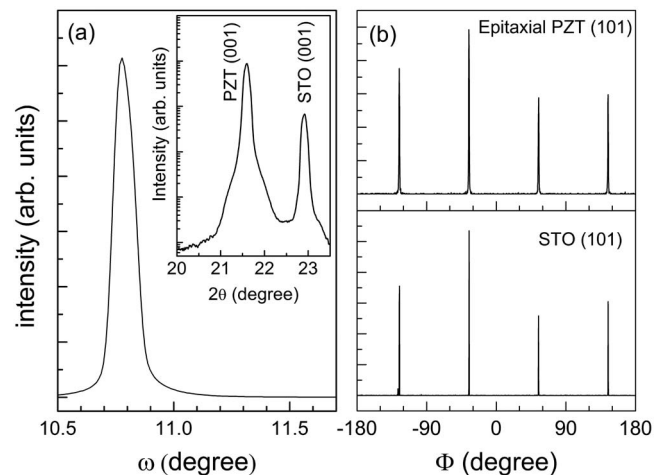


FIG. 1. (a) HRXRD ω rocking curve of the (001) PZT reflection. Inset is a 2θ - ω scan of the epitaxial PZT film on a STO substrate. (b) Φ scan pattern of asymmetrical (101) reflection of epitaxial PZT film (upper panel) and STO substrate (lower panel).

^{a)}Electronic mail: xiaob@vcu.edu.

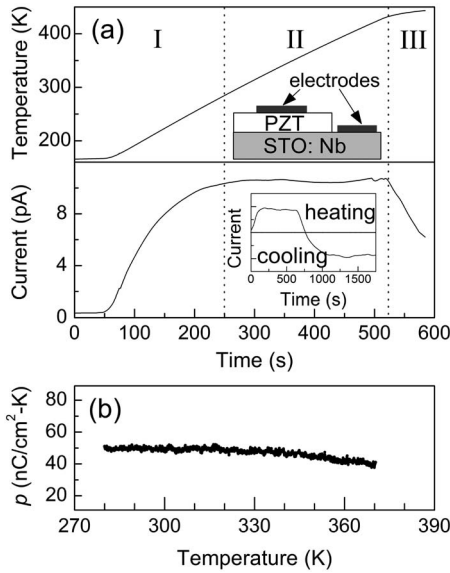


FIG. 2. (a) Pyroelectric current response with changing temperature as a function of time. (b) Temperature dependence of pyroelectric coefficient of the PZT/STO: Nb heterostructure. The inset shows current variation for the whole cooling-heating cycle.

ing to the international center for diffraction data⁸). The corresponding c lattice parameter is 4.136 Å. To determine the in-plane lattice parameter a , we performed 2θ - ω scans of the asymmetric (101) reflection, which was located at 30.95° , corresponding to $a=4.031$ Å. The obtained lattice parameters of $c=4.136$ and $a=4.031$ are very close to those in bulk PZT crystals of the MPB composition, 4.146 and 4.036 Å, respectively.⁸ Our findings suggest that 300 nm thick PZT thin films grown on STO substrates are nearly fully relaxed. The HRXRD ω -rocking curve measurements were performed to evaluate the crystal quality of PZT films [see Fig. 1(a)]. The full widths at half maximum of rocking curves were 4.2 and 30 arc min for the symmetric (001) and for the asymmetric (101) reflections, respectively, indicating high crystal quality. To determine the in-plane epitaxial relationship of the PZT/STO heterostructure, Φ scans of asymmetrical (101) reflection were performed separately for the PZT film and the STO substrate. The observed fourfold rotational symmetry [see Fig. 1(b)] clearly implies an in-plane epitaxial relationship of PZT[100]||STO[100].

The PZT films grown on conductive STO substrates doped with Nb to 0.5 wt % (resistivity ~ 0.05 Ω -cm) were used to characterize the electrical properties of the material. Capacitor structures composed of 50/30-nm-thick Au/Cr circular electrodes of 200 μ m in diameter were fabricated on top of PZT films. The bottom electrodes of PZT capacitors were placed on top of the STO substrate, as shown in the inset of Fig. 2(a). Using the fabricated capacitor structures, pyroelectric properties of PZT thin films were studied by the Byer-Roundy method.⁹ A computer-controlled measurement setup consisting of an HP 4142B modular dc source/monitor and a Lakeshore 331 temperature controller was assembled for measuring the pyroelectric response. The sample under test was placed on a copper plate in a heating chamber equipped with an electrical heater and a liquid-nitrogen cooler, which was poled at room temperature with an electric field of 500 kV/cm. During the pyroelectric response measurements, the chamber pressure was kept around 10^{-2} Torr.

The temperature was ramped up from 160 to 420 K with a rate of ~ 0.6 K/s. The current induced by temperature change was measured every 200 ms. As demonstrated in Fig. 2(a), this current gradually increases in region I, at the beginning of the temperature ramping, and then reaches a steady-state value in region II. The gradual current increase cannot be considered as the actual pyroelectric response because it is mainly caused by charging the parasitic capacitances in the measurement circuit.

As shown in Fig. 2(a), as the heating rate was reduced in region III, the induced current decreased accordingly. To some extent, this reduction includes the discharging current from the parasitic capacitances. Hence, the pyroelectric coefficient was calculated only for region II using $p(T) = I(AdT/dt)^{-1}$, where I is the current induced by the pyroelectric effect, A is the capacitor area, and dT/dt is the temperature ramping rate. The magnitude of p was also extracted from the cooling [the inset of Fig. 2(a) presents the full heating-cooling cycle]. To eliminate the possible contribution from other thermally stimulated currents, especially those associated with charging/discharging electron traps present in the material where these currents tend to be unidirectional, we averaged pyroelectric coefficients extracted separately for the heating and cooling cycles. Figure 2(b) shows the magnitude of p , averaged at the temperature ranging from 280 to 370 K. At room temperature, the measured magnitude of p for PZT thin films grown on STO: Nb was 48 nC/cm² K, which are larger than those reported for highly oriented PZT (Ref. 10) (26 nC/cm² K) and comparable to Sm-doped¹¹ (45 nC/cm² K), Mn-doped¹² (35 nC/cm² K), and Mn-codoped and Sb-codoped PZT (Ref. 13) (45 nC/cm² K) thin films and PZT-based pyroelectric ceramics¹⁴ (35–40 nC/cm² K). The large pyroelectric coefficient observed in our samples is likely due to the high crystal quality of the PZT films on closely lattice-matched STO substrates. The weak temperature dependence in the range from 280 to 370 K implies that the pyroelectricity of the PZT/STO: Nb structure is dominated by the transient, temperature-induced polarization change. In addition, F_D , the figure of merit derived from specific detectivity, was evaluated: $F_D = p/[c'(\epsilon\epsilon_0 \tan \delta)^{1/2}]$, where c' is the volume specific heat ($c' = 2.7 \times 10^6$ J m⁻³ K⁻¹ for PZT thin films), ϵ is the relative permittivity, ϵ_0 is the vacuum permittivity, $\tan \delta$ is the dielectric loss, and p is the pyroelectric coefficient.^{12,15} The values of F_D were found to be $(1.89\text{--}2.60) \times 10^{-5}$ Pa^{-0.5} at 30 Hz, where ϵ is 310 and $\tan \delta$ is 0.017 extracted from capacitance-voltage measurements at room temperature.

The ferroelectric properties of the PZT films were examined by polarization-electric field (P - E) measurements at different temperatures. Prior to the P - E measurements, we examined I - V characteristics on the PZT films at different temperatures. At an applied electric field of 500 kV/cm, leakage current densities as low as 1×10^{-8} and 5×10^{-8} A/cm² were observed at 300 and 400 K, respectively, indicating high dielectric property. At room temperature, the remanent polarization was around 45–58 μ C/cm², slightly varying among the devices measured. The P - E curves of a PZT/STO: Nb heterostructure measured at 260 and 360 K are shown in Fig. 3, indicating a temperature dependence of the remanent polarization. The relationship of the ferroelectric polarization and temperature can be ex-

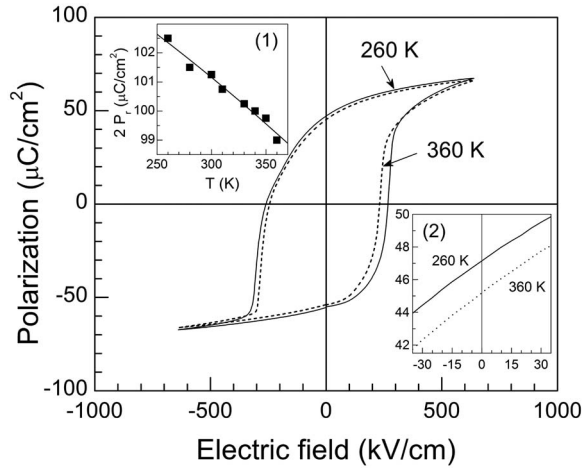


FIG. 3. P - E hysteresis loops of a PZT thin film on Nb-doped STO substrate measured at 260 K (dashed) and 360 K (solid). Inset (1) shows the temperature dependence of remanent polarization in the PZT films. Inset (2) is a close up of the $+P_r$ region.

pressed by the Landau–Devonshire theory as¹⁶ $P_S = \sqrt{a_0(T_0 - T)/b}$, where a_0 and b are the coefficients of the free energy polynomial expansion, P_S is the spontaneous polarization, and T_0 is the phase transition temperature ($T_0 \approx T_C$, T_C is the Curie temperature). For $T < T_0$, the polarization decreases as temperature increases in relation to the pyroelectric effect. At a constant external electric field, the pyroelectric coefficient can be expressed as $p = dP_S/dT$. The same trend can be obtained by measuring the temperature dependence of the remanent polarization P_r , which, in principle, can be used for estimating the pyroelectric coefficient. For our PZT films, the magnitude of p estimated from temperature-dependent P - E measurements ranges from 10 to 60 nC/cm² K. However, this approach has some limitations and results in relatively large experimental error. In fact, the value of spontaneous polarization in PZT is about a thousand times larger than that caused by the pyroelectric effect. A more significant limitation is related to the asymmetry of the hysteresis loops (see Fig. 3). This asymmetry could be a manifestation of the built-in field in a heterostructure, which may also be temperature dependent, and introduces a large uncertainty into the value of p extracted from the P - E measurements as the zero applied external field no longer corresponds to zero net field. This asymmetry phenomenon was reported for various heterostructures, such as

PZT/SiO₂/Si,¹⁷ PZT/GaN,¹⁸ and PZT/STO.¹⁹ In addition, dissimilar electrodes, mobile charges, and interface charge traps are also considered as possible sources of the observed asymmetry. The lack of detailed experimental results makes it difficult to quantify their individual contributions to the asymmetry.

In conclusion, high-quality epitaxial PZT thin films have been grown on STO(001) substrates by off-axis rf magnetron sputtering. The formation of (001)-oriented perovskite phase has been revealed by HRXRD. The pyroelectric properties of the PZT films have been studied as a function of temperature in the range from 280 to 370 K. The measurements have yielded a pyroelectric coefficient as high as 48 nC/cm² K at room temperature.

This work was supported by a grant from the Office of Naval Research under the direction of Dr. Ingham Mack, preceded by Dr. C. E. C. Wood.

- ¹N. Izyumskaya, Y.-I. Alivov, S.-J. Cho, H. Lee, Y.-S. Kang, and H. Morkoç, *Crit. Rev. Solid State Mater. Sci.* **32**, 111 (2007).
- ²P. Murali, *J. Micromech. Microeng.* **10**, 136 (2000).
- ³M. Kohli, C. Wuethrich, K. Brooks, B. Willing, M. Forster, P. Murali, N. Setter, and P. Ryser, *Sens. Actuators, A* **60**, 147 (1997).
- ⁴N. M. Shorrocks, A. Patel, M. J. Walker, and A. D. Parsons, *Microelectron. Eng.* **29**, 59 (1995).
- ⁵S. B. Lang, *Phys. Today* **58**(8), 31 (2005).
- ⁶W. Gong, J.-F. Li, X. Chu, Z. L. Gui, and L. T. Li, *Appl. Phys. Lett.* **85**, 3818 (2004).
- ⁷H. Nonomura, H. Fujisawa, and M. Shimizu, *Jpn. J. Appl. Phys., Part 1* **41**, 6682 (2002).
- ⁸JCPDS-ICDD Card No. 330784 (unpublished).
- ⁹R. L. Byer and C. B. Roundy, *Ferroelectrics* **3**, 333 (1972); *IEEE Trans. Sonics Ultrason.* **SU-19**, 333 (1972).
- ¹⁰J. Wu, J. Zhu, D. Xiao, J. Zhu, J. Tan, and Q. Zhang, *J. Appl. Phys.* **101**, 094107 (2007).
- ¹¹A. K. Tripathi, T. C. Goel, and C. Prakash, *Mater. Sci. Eng., B* **96**, 19 (2002).
- ¹²Q. Zhang and R. W. Whatmore, *J. Appl. Phys.* **94**, 5228 (2003).
- ¹³A. Ignatiev, Y. Q. Xu, N. J. Wu, and D. Liu, *Mater. Sci. Eng., B* **56**, 191 (1998).
- ¹⁴R. W. Whatmore, Q. Zhang, C. P. Shaw, R. A. Dorey, and J. R. Alcock, *Phys. Scr., T* **129**, 6 (2007).
- ¹⁵R. W. Whatmore, *Rep. Prog. Phys.* **49**, 1335 (1986).
- ¹⁶P. Chandra and P. B. Littlewood, in *Physics of Ferroelectrics: A Modern Perspective*, edited by K. Rabe, Ch. H. Ahn, and J.-M. Triscone (Springer, Berlin, 2007), p. 87.
- ¹⁷Y. Lin, B. R. Zhao, H. B. Peng, Z. Hao, B. Xu, Z. X. Zhao, and J. S. Chen, *J. Appl. Phys.* **86**, 4467 (1999).
- ¹⁸B. Xiao, X. Gu, N. Izyumskaya, V. Avrutin, J.-Q. Xie, and H. Morkoç, *Appl. Phys. Lett.* **91**, 182908 (2007).
- ¹⁹Z.-X. Zhu, J.-F. Li, F.-P. Lai, Y. Zhen, Y.-H. Lin, C.-W. Nan, and L. Li, *Appl. Phys. Lett.* **91**, 222910 (2007).